

Received April 12, 2020, accepted April 30, 2020, date of publication May 12, 2020, date of current version May 22, 2020.

Digital Object Identifier 10.1109/ACCESS.2020.2994029

Identification of Air-Fuel Ratio for a High-Temperature and High-Speed Heat-Airflow Test System Based on Support Vector Machine

CHAOZHI CAI^{ID}, LUBIN GUO, AND YUMIN YANG

School of Mechanical and Equipment Engineering, Hebei University of Engineering, Handan 056038, China

Corresponding author: Chaozhi Cai (caichaozhi1983@163.com).

This work was supported in part by the Nature Science Foundation of Hebei Province under Grant E2017402037 and Grant E2020402060, and in part by the Science and Technology Research Project of Hebei Province under Grant ZD2018012.

ABSTRACT Air-fuel ratio is an important parameter in high-temperature and high-speed heat-airflow test system. If air-fuel ratio of the system is too low, the fuel cannot be fully burned, which will not only reduce the control performance of the gas temperature, but also increase the pollutant emissions of the combustor. In order to solve this problem, it is necessary to identify the air-fuel ratio of the system, get the prediction model of the air-fuel ratio, and adjust the fuel input according to the prediction value of the air-fuel ratio. In order to realize the accurate identification of the air-fuel ratio of the system, this paper briefly analyses the mathematical model of the air-fuel ratio in high-temperature and high-speed heat-airflow test system, and proposes an identification method of the air-fuel ratio based on support vector machine. On the basis of the experimental data, the air-fuel ratio of the system is identified by using different kernels, i.e. firstly, the experimental scheme is designed, and the fuel mass flow rate, air mass flow rate, gas temperature and actual air-fuel ratio of the system are collected under different experimental conditions; then, the collected data are divided into training datasets and test datasets, and the training datasets are trained by support vector machine to obtain identification model of the air-fuel ratio; finally, the identification model is validated with test datasets under different conditions, and the accuracy of the model is obtained. The identification results show that the support vector machine has good identification performance and can accurately approximate the actual dynamic process of the air-fuel ratio. The average absolute error of the identification model is less than 0.05, and the average relative error is less than 0.5% when the test datasets are smaller than the training datasets.

INDEX TERMS High-temperature, high-speed, combustion system, air-fuel ratio, support vector machine, system identification.

I. INTRODUCTION

The high-temperature and high-speed heat-airflow test system (HHHTS) is a key basic technical equipment in the field of aerospace. It can not only be used in the test and research of thermal components in thermal machinery, high-speed aircraft and aero engine, but also can be used in the static and dynamic thermal calibration of high temperature sensors in aero engine development. It involves basic theories and key technologies such as fluid fuel delivery and control, combustion and temperature control. Its performance

The associate editor coordinating the review of this manuscript and approving it for publication was Quan Zou^{ID}.

level not only directly restricts the development level of national key aero engine, but also affects the reliability of static and dynamic calibration of high-temperature sensors and the safety of high-speed aircraft [1], [2]. The control performance of the gas temperature is an important index to measure the performance level of the HHHTS. However, in actual gas temperature control, especially in low speed and high temperature conditions, fuel combustion is often inadequate due to the decrease of air-fuel ratio, which will not only affect the control performance of the gas temperature, but also increase the pollution of the combustor. Emissions of pollutants are not conducive to energy conservation and emission reduction, this is the so-called fuel-rich combustion

phenomenon. In order to solve this problem, it is necessary to identify the air-fuel ratio of the system, get the prediction model of the air-fuel ratio, and then adjust the fuel input according to the predicted value of the air-fuel ratio, so as to avoid the phenomenon of the fuel-rich combustion, improve the control performance of the gas temperature, and achieve the purpose of energy saving and emission reduction.

Air-fuel ratio is an important index affecting the emission, power and economy of the engine [3]–[5]. The accurate mathematical model of the air-fuel ratio is the basis for the accurate control of the air-fuel ratio of the engine [6]. In order to obtain an accurate mathematical model of the engine's air-fuel ratio, many scholars have conducted in-depth research. Aquilto first proposed the average air-fuel ratio model [7]. Cho *et al.* proposed a multi-point injection air-fuel ratio model of the engine for control system development [8]. Hendricks *et al.* proposed a three-state dynamic average air-fuel ratio model [9]. Although the above mentioned mechanism models have important significance in the modeling of the engine's air-fuel ratio, due to the complexity of the model itself, the above models have their own limitations, and the accuracy of the above models will become worse in some cases. In order to improve the modeling accuracy of the engine's air-fuel ratio, many scholars have done a lot of in-depth research on the identification of the engine's air-fuel ratio. In order to establish the air-fuel ratio model of the gasoline engine under transitional conditions, Hou *et al.* proposed an identification method for the air-fuel ratio under transitional conditions based on Elman neural network [10]. Based on the average model of the engine's air-fuel ratio, Chen *et al.* identified the uncertain parameters in the model by using least square method [11]. In order to establish an accurate mathematical model of the engine's air-fuel ratio, Li *et al.* proposed a method of structure identification of the non-linear model [12]. In order to overcome the influence of non-linear characteristics of the ignition engine on the air-fuel ratio, Saraswati *et al.* identified the air-fuel ratio of the ignition engine by using recurrent neural network [13]; Shi *et al.* established an accurate model of the air-fuel ratio of the ignition engine by using RBF network [14]; In order to overcome the influence of multi-dimensional non-linearity characteristics on the air-fuel ratio of the gasoline engine, Xu *et al.* proposed an identification method of the air-fuel ratio based on opportunistic chaotic support vector machine [15]. In order to control the air-fuel ratio accurately, Zhai *et al.* used the neural network to identify the air-fuel ratio of the ignition engine, and used the identified air-fuel ratio as the feedback of the control system, thus constituting the soft sensor of the air-fuel ratio [16].

From the above literatures, it can be seen that the model research of the air-fuel ratio mainly focuses on the engine. So far, there is no report on the research of the air-fuel ratio model of the HHHTS. Although the study object is air-fuel ratio, The HHHTS is quite different from the engine in structure, working principle and function, so its air-fuel ratio model will also be quite different from the engine's

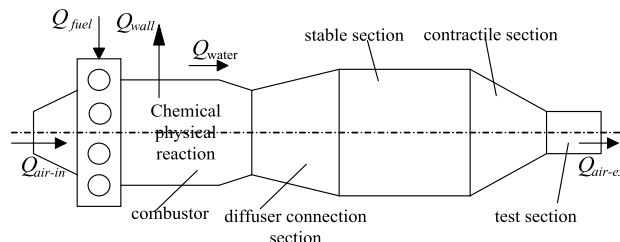


FIGURE 1. The structure and principle of the system.

air-fuel ratio model. Therefore, the air-fuel ratio model of the engine cannot be directly applied to the system. In order to predict the air-fuel ratio of the HHHTS, an appropriate identification method must be proposed. At present, the popular system identification methods mainly include artificial neural network [17], [18], fuzzy logic [19], [20], genetic algorithm [21], [22], wavelet analysis [23], [24] and support vector machine (SVM) [25], [26]. Compared with other identification methods, SVM not only has the advantages of simple algorithm, good robustness and strong generalization ability, but also shows many unique advantages in solving the problem of limited sample and nonlinear identification [27], which is more suitable for the air-fuel ratio identification of the HHHTS. Therefore, this paper introduced SVM to propose an air-fuel ratio identification method based on SVM. That is to say, SVM is used to identify the air-fuel ratio of the system according to the input and output data of the system.

II. MATHEMATICAL MODEL OF THE AIR-FUEL RATIO

A. WORKING PRINCIPLE OF THE SYSTEM

The main structure and composition diagram of the HHHTS is shown in Fig.1. It can be seen from the figure that the system consists of a combustor, a diffuser connection section, a stable section, a contractile section and a test section. Its working principle is that: firstly, high-speed air flow and fuel burn in the combustor to generate high temperature and high speed gas flow; then the high temperature and high speed gas flow passes through the diffuser connection section, the stable section and the contractile section to form a stable and uniform temperature field in the test section; finally, the specimen is placed in the test section to complete the test and obtain the test results. In addition to the above core parts, in order to make the system work properly, it is equipped with a measurement subsystem, a control subsystem, a fuel supply subsystem, a cooling subsystem and a gas supply subsystem, etc.

B. MODEL ANALYSIS OF THE AIR-FUEL RATIO

The air-fuel ratio model block diagram of the HHHTS is shown in Fig. 2. It can be seen from the figure that fuel and air enter the combustor through the fuel supply channel and gas supply channel respectively. The actual air-fuel ratio is equal to the ratio of the air mass flow rate m_{ac} to the fuel mass flow rate m_{fc} entering the combustor, that is, the actual

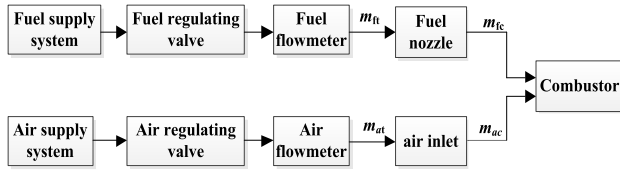


FIGURE 2. The air-fuel ratio model block diagram of the HHHTS.

air-fuel ratio can be expressed as follows

$$AFR = \frac{m_{ac}}{m_{fc}} \tag{1}$$

The air supply channel is composed of an air supply system, an air regulating valve, an air flowmeter and an air inlet. The high-speed air generated by the air supply system enters the combustor of the system after passing through the control valve, air flowmeter and air inlet. Assuming that the air velocity in the pipeline is uniform and stable under normal working conditions, it can be considered that the air mass flow rate m_{ac} enters the combustor is equal to the air mass flow rate passes through the air flowmeter m_{at} . That is to say $m_{ac} = m_{at}$.

The fuel supply channel consists of a fuel supply system, a fuel control valve, a fuel flowmeter and a fuel nozzle. The fuel produced by the fuel supply system passes through the fuel regulating valve, fuel flowmeter, and then enters the combustor of the system through the fuel nozzle. The fuel mass flow rate m_{ft} which enters the fuel nozzle (which can be measured by the fuel flowmeter) can be divided into two parts after it is ejected from the nozzle, one part is the fuel vapor which can directly enter the combustor, the other part is deposited on the wall in the form of liquid droplets to form an oil film, and the fuel in the film evaporates continuously, and the evaporated fuel vapor enters the combustor together with the previous part of the fuel vapor. This shows that the actual fuel mass flow rate enters the combustor m_{fc} is not the same as that passes through the fuel flowmeter m_{ft} . Therefore, the actual air-fuel ratio of the system is not equal to the ratio of the air mass flow rate measured by the air flowmeter to the fuel mass flow rate measured by the fuel flowmeter.

According to reference [28], the dynamic model of oil film can be expressed as follows

$$m_{fv} = m_{ft}(1 - x) \tag{2}$$

$$\dot{m}_{ff} = \frac{1}{\tau}(-m_{ff} + m_{ft}q) \tag{3}$$

$$m_{fc} = m_{fv} + m_{ff} \tag{4}$$

where m_{fv} is the mass flow rate of the fuel vapor; m_{ft} is the mass flow rate of the fuel ejected from nozzle; x is the fuel deposition coefficient; m_{ff} and \dot{m}_{ff} are the mass and velocity of the fuel film evaporation; m_{fc} is the mass flow rate of the fuel entering the combustor; τ is the time coefficient of the fuel evaporation; q is the fuel distribution coefficient. τ and q are non-linear functions of the combustor temperature. Therefore, the mass flow rate of fuel entering the

combustor is a non-linear function of the gas temperature T and m_{ft} . It can be expressed as follows

$$m_{fc} = f_1(m_{ft}, T) \tag{5}$$

where f_1 is a non-linear function.

According to the equation (1) and (5), the mathematical model of the air-fuel ratio of the system can be described by the following non-linear functions

$$AFR = f_2(m_{at}, m_{ft}, T) \tag{6}$$

where f_2 is a non-linear function.

Therefore, the actual air-fuel ratio of the system can be identified by the data of the air mass flow rate, fuel mass flow rate and gas temperature of the combustor obtained by sensors.

III. SUPPORT VECTOR REGRESSION

A. BASIC PRINCIPLE OF SVR

Support Vector Machine (SVM) is a classification algorithm for classical classification problems. Support Vector Regression (SVR) is the application of the SVM in the field of functional regression. Assuming that the input and output sample datasets of the system to be identified are $\{x_i, y_i\}$, where $i = 1, \dots, l$, $x_i \in R_n$ is the input vector of the n -dimensional system and $y_i \in R_n$ is the output of the system, the identification system of SVR is to determine a function f through data training, satisfying that for any input x , the corresponding output y can be found in the range of accuracy. SVM method uses the non-linear mapping function $\phi(\cdot)$ to map the sample nonlinearly to the high-dimensional feature space, thus transforming the problem of estimating the non-linear function into the problem of estimating the linear function in the high-dimensional feature space. It can be expressed as

$$f(x) = \omega^T \phi(x) + b \tag{7}$$

The core of the above regression problem is to solve parameters ω and b . According to the principle of structural risk minimization, finding parameters ω and b can be equivalent to solving the following optimization problem

$$\min_{\omega, b} J = \frac{1}{2} \omega^T \cdot \omega \tag{8}$$

$$st \begin{cases} y_i - \omega^T \phi(x_i) - b \leq \varepsilon \\ \omega^T \phi(x_i) + b - y_i \leq \varepsilon \end{cases} \tag{9}$$

In order to determine the solution of the above optimization problem, the slack variables ξ_i and ξ_i^* are introduced, and then the optimization problem can be transformed into the following problem

$$\min_{\omega, b, \xi, \xi^*} J = \frac{1}{2} \omega^T \cdot \omega + C \sum_{i=1}^l (\xi_i + \xi_i^*) \tag{10}$$

$$st \begin{cases} y_i - \omega^T \phi(x_i) - b \leq \varepsilon + \xi_i \\ \omega^T \phi(x_i) + b - y_i \leq \varepsilon + \xi_i^* \\ \xi_i, \xi_i^* \geq 0 \end{cases} \tag{11}$$

Through the constraints of equation (11), ω and b in the objective function can be obtained by minimizing equation (10). $\frac{1}{2}\omega^T \cdot \omega$ in equation (10) is the regularization part, which can improve generalization ability, while the latter one in equation (10) is used to reduce errors, and C ($C > 0$) is the penalty coefficient. The optimal solution can be obtained by the dual form of equation (10). By introducing the Lagrangian function, it can be obtained

$$\begin{aligned}
 L(\omega, b, \xi, \xi^*, \alpha, \alpha^*, \eta, \eta^*) &= \frac{1}{2}\omega^T \cdot \omega + C \sum_{i=1}^l (\xi_i + \xi_i^*) \\
 &\quad - \sum_{i=1}^l \alpha_i [\varepsilon + \xi_i - y_i + (\omega^T \phi(x_i) + b)] \\
 &\quad - \sum_{i=1}^l \alpha_i^* [\varepsilon + \xi_i^* + y_i - (\omega^T \phi(x_i) - b)] \\
 &\quad - \sum_{i=1}^l (\eta_i \xi_i + \eta_i^* \xi_i^*) \tag{12}
 \end{aligned}$$

where $\alpha, \alpha^*, \eta, \eta^* \geq 0$ are Lagrangian multiplier. The form of dual problem can be obtained by minimizing function L to ω, b, ξ, ξ^* and maximizing L to $\alpha, \alpha^*, \eta, \eta^*$, and substituting kernel function for non-linear mapping, i.e. substituting $K(x, x') = \langle \phi(x), \phi(x') \rangle$ for $\phi(\cdot)$.

$$\begin{aligned}
 \max_{\alpha, \alpha^*} J &= -\frac{1}{2} \sum_{i,j=1}^l (\alpha_i - \alpha_i^*)(\alpha_j - \alpha_j^*)K(x_i, x_j) \\
 &\quad - \varepsilon \sum_{i=1}^l (\alpha_i + \alpha_i^*) + \sum_{i=1}^l y_i(\alpha_i - \alpha_i^*) \tag{13}
 \end{aligned}$$

$$\text{st} \begin{cases} \sum_{i=1}^l (\alpha_i - \alpha_i^*) = 0 \\ \alpha_i, \alpha_i^* \in [0, C] \end{cases} \tag{14}$$

For linear systems, linear kernel function $K(x_i, x) = (x_i \cdot x)$ is used to the structural parameters of the identification system; for non-linear systems, polynomial kernel function and radial basis function (rbf) kernel function are used. It can be written as

$$K(x_i, x) = (x_i \cdot x + d)^p \tag{15}$$

$$K(x_i, x) = \exp(-\|x - x_i\|^2 / \sigma^2) \tag{16}$$

To solve the quadratic programming problem, the following equation can be obtained

$$w = \sum_{i=1}^l (a_i - a_i^*)\phi(x_i) \tag{17}$$

According to the KKT condition, the following results can be obtained at the optimal solution

$$\begin{cases} a_i(\varepsilon + \xi_i - y_i + \sum_{i=1}^l (a_i - a_i^*)K(x_i, x) + b) = 0 \\ a_i^*(\varepsilon + \xi_i^* + y_i - \sum_{i=1}^l (a_i - a_i^*)K(x_i, x) - b) = 0 \end{cases} \tag{18}$$

$$\begin{cases} (C - a_i)\xi_i = 0 \\ (C - a_i^*)\xi_i^* = 0 \end{cases} \tag{19}$$

From the above results, it can be concluded that when the sample point is located in the insensitive area, $a_i = 0$ and $a_i^* = 0$, when the sample point is located outside, $a_i = 0$ or $a_i^* = 0$, and when the sample point is on the boundary, $\xi_i = 0$ and $\xi_i^* = 0$, so a_i and a_i^* belong to C . Therefore, the calculation formula of b can be obtained as follows

$$\begin{cases} b = y_i - \sum_{i=1}^l (a_i - a_i^*)K(x_i, x) - \varepsilon & a_i \in (0, C) \\ b = y_i - \sum_{i=1}^l (a_i - a_i^*)K(x_i, x) + \varepsilon & a_i^* \in (0, C) \end{cases} \tag{20}$$

The samples corresponding to $a_i \neq 0$ and $a_i^* \neq 0$ are called support vectors, so the following equation can be obtained

$$w = \sum_{i=1}^l (a_i - a_i^*)\phi(x_i) = \sum_{i \in SVs} (a_i - a_i^*)\phi(x_i) \tag{21}$$

where SVs represents the set of support vectors, so $f(x)$ can be expressed as

$$f(x) = \sum_{i \in SVs} (a_i - a_i^*)K(x_i, x) + b \tag{22}$$

B. PARAMETER IDENTIFICATION PROCESS BASE ON SVM

In order to better understand how SVM realizes parameter identification, based on the introduction of the basic principle of the SVM identification in the last section, this paper takes the air-fuel ratio identification of the HHHTS as an example to introduce the process of the parameter identification based on SVM. The process of the parameter identification based on SVM is as follows.

(1) Determine the parameters that need to be identified and other parameters that affect the parameters, that is, determine the input and output parameters of the identified system, and on this basis, build an experimental system for data collection, get the input and output sample datasets $\{x_i, y_i\}$ of the identified system, and divide the datasets into training datasets and test datasets. Firstly, the parameter needed to be identified in this paper is the air-fuel ratio of the HHHTS. In addition, from Section II.B, it can be seen that the air-fuel ratio is a non-linear function of the air mass flow rate m_{at} , fuel mass flow rate m_{ft} and gas temperature T in the combustor. Therefore, m_{at} , m_{ft} and T are the input parameters of the system when identifying the air-fuel ratio, and their sample data can form the input datasets $\{x_i\}$; The air-fuel ratio is the output parameter of the system, and its sample data can form the output datasets $\{y_i\}$.



FIGURE 3. Experimental setups.

(2) The training datasets are used to train the identification model and get the model of the identified system. Firstly, select the appropriate precision parameter ε , penalty coefficient C and kernel function $K(x, x')$ to solve the dual optimization problem described in equation (13) and get parameter $a = (a_1, a_1^*, \dots, a_l, a_l^*)$; then select a positive component of a to calculate the value of b by using equation (20); finally, according to equation (22), the identification model of the air-fuel ratio can be obtained.

(3) The test datasets are used to verify the identification model of the air-fuel ratio obtained in the second step, and the accuracy of the identification model of the air-fuel ratio can be obtained. Firstly, determine the evaluation criteria of the inspection accuracy, such as mean square error, root mean square error, average absolute error and average relative error; then, substitute the input data in the test datasets into the air-fuel ratio identification model to get the identified air-fuel ratio; finally, compare the actual collected air-fuel ratio with the identified air-fuel ratio to get the validation accuracy.

IV. IDENTIFICATION OF THE AIR-FUEL RATIO BASED ON SVM

A. EXPERIMENTAL SETUPS

In order to realize the identification of the air-fuel ratio of the HHHTS, based on the existing hardware of the fuel supply subsystem and air supply subsystem, the measurement and control system based on the field PLC controller and remote industrial computer was developed. The experimental setups are shown in Fig.3. It can be seen from the figure that the experimental setups consist of the test system body and the measurement control system. The main body of the test system provides the basic conditions for the experiment. The measurement control system is used to realize the automatic control and measurement of the air mass flow rate, fuel mass flow rate, gas temperature and actual air-fuel ratio. The fuel mass flow rate is obtained by the fuel flowmeter, the air mass flow rate is obtained by the air flowmeter, the gas temperature is obtained by the thermocouple, and the actual air-fuel ratio is obtained by Bosch Lsu4.9 oxygen sensor.

TABLE 1. The sample data range of the HHHTS.

parameter	m_{ft} (g/s)	m_{at} (g/s)	T (°C)	AFR
max	12.03	156.9	907.5	25.93
min	5.95	155.2	551.6	12.48

B. EXPERIMENTAL SCHEME AND DATA PREPROCESSING

From the analysis of the air-fuel ratio model of the HHHTS in Section II.B, it can be seen that air-fuel ratio is the non-linear function of the air mass flow rate m_{at} , fuel mass flow rate m_{ft} and gas temperature T in combustor, so air-fuel ratio can be identified by obtaining the experimental data of m_{at} , m_{ft} and T . Because the general work flow of the HHHTS is: firstly, the air mass flow rate of the system is adjusted to a fixed value (the Mach number condition of the system is obtained), and then the gas temperature is controlled by adjusting the fuel mass flow rate. Therefore, it is necessary to fix the air mass flow rate on a certain value first, then change the fuel mass flow rate, and collect m_{at} , m_{ft} , T and the actual air-fuel ratio at the same time.

The HHHTS has many working conditions, but they are basically similar, except that the air mass flow rate is different (namely the Mach number of the system is different). In order to verify the validity of the identification method of the air-fuel ratio, two kind of experiments were carried out when the system's Mach number is equal to 0.2 ($m_{at} = 156$ g/s). Experiment 1 is a gas temperature rise test, that is, when the air mass flow rate is equal to 156 g/s, the fuel mass flow rate is increased from 6 g/s to 12 g/s at different time (10s, 15s, 20s), and the sampling time is 0.01s, so a total of 4500 sets of test data were obtained. Experiment 2 is a gas temperature drop test, i.e. when the air mass flow rate is equal to 156 g/s, the fuel mass flow rate is reduced from 12 g/s to 6 g/s in different time (10s, 15s, 20s), and the sampling time is 0.01s, also a total of 4500 sets of test data were obtained. Taking the 15 s datasets as training samples, and the 10 s and 20 s datasets were tested respectively after the SVM training was completed. The main reason of choosing 10s and 20s datasets for identification is that the response time of the fuel control subsystem is required to be in the range of 10 s to 20 s, so as to ensure the rapid response of the whole system. Because the values of sample datasets in different dimensions are quite different, normalization is needed before identification. Table 1 shows the sample datasets range of the HHHTS.

C. AIR-FUEL RATIO IDENTIFICATION

Section II.B shows that the air-fuel ratio of the HHHTS is a non-linear function of m_{at} , m_{ft} and T . Therefore, when using SVM to identify the air-fuel ratio, a non-linear kernel function should be selected. In this paper, in order to find the proper kernel function and get good identification accuracy, based on the measured curve of the air-fuel ratio, the identification of the air-fuel ratio was studied under the condition of choosing polynomial kernel function and radial basis function (rbf)

TABLE 2. Training accuracy under temperature rise condition.

kernel	mse	rmse	mae	mre
poly(15s)	0.0013	0.0363	0.028	0.12%
rbf(15s)	0.0028	0.0529	0.0434	0.19%

TABLE 3. Verification accuracy under temperature rise condition.

kernel	mse	rmse	mae	mre
poly(10s)	0.0014	0.0377	0.0298	0.13%
poly(20s)	0.169	0.411	0.311	1.41%
rbf(10s)	0.0032	0.0566	0.0428	0.19%
rbf(20s)	0.165	0.407	0.284	1.28%

kernel function respectively. The air-fuel ratio identification program in this paper was implemented by Scikit-Learn, and SVR function was used as SVM to realize the identification of the air-fuel ratio. Because the characteristics of the air-fuel ratio are different when the temperature rises and falls, the air-fuel ratio of the system was identified under two different conditions.

1) IDENTIFICATION UNDER TEMPERATURE RISE CONDITION

Under this condition, firstly, 1500 sets of the test data with a temperature rise of 15s were used as training samples to identify the air-fuel ratio of the system, and then the identified model was validated by using 10s and 20s datasets respectively. When using polynomial kernel function, the parameters of the SVM were: kernel = “poly”, “degree = 3”, gamma = 1, coef 0 = 14, C = 10; when using radial basis kernel function, the parameters of the SVM were: kernel = “rbf”, “gamma = 0.25”, C = 10. Mean square error (mse), root mean square error (rmse), mean absolute error (mae) and mean relative error (mre) were used as the criteria to evaluate the accuracy of the identification model. The training and verification accuracy of the air-fuel ratio based on SVM under two kinds of kernels were obtained as shown in table 2 and table 3.

In addition, by exporting the training output data and the verification output data of the SVM, the air-fuel ratio identification results can be obtained as shown in Fig. 4, Fig. 5 and Fig. 6 (The figures were obtained by selecting the data with the highest accuracy in table 2 and table 3).

2) IDENTIFICATION UNDER TEMPERATURE DROP CONDITION

Under this condition, firstly, the air-fuel ratio of the system was identified by using 1500 sets of the test data with temperature drop of 15s as training samples, and then the identified model was validated by using 10s and 20s datasets respectively. The parameters of the SVM were consistent with the temperature rise condition. Using the same parameters as the accuracy test standard, the training accuracy and verification

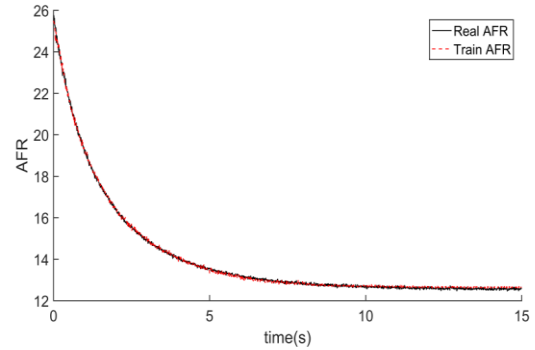


FIGURE 4. Training results of the air-fuel ratio under temperature rise condition.

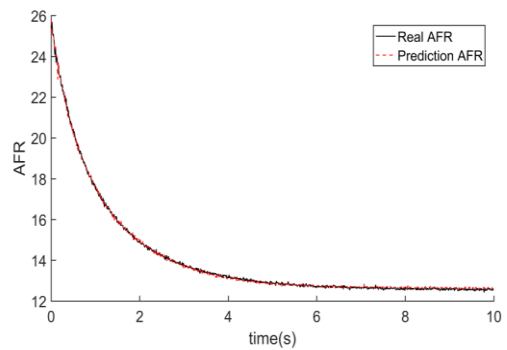


FIGURE 5. Validation results of the air-fuel ratio of 10s test datasets under temperature rise condition.

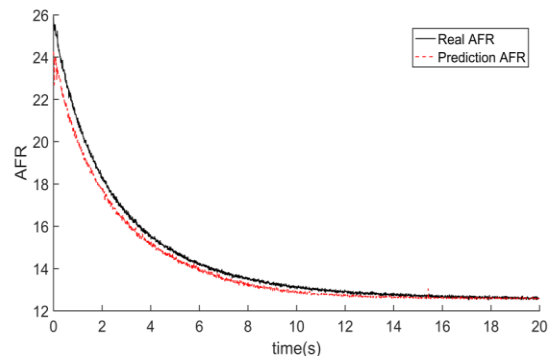


FIGURE 6. Validation results of the air-fuel ratio of 20s test datasets under temperature rise condition.

TABLE 4. Training accuracy under temperature drop condition.

kernel	mse	rmse	mae	mre
poly(15s)	0.0017	0.041	0.034	0.24%
rbf(15s)	0.0032	0.0564	0.0476	0.34%

accuracy of the air-fuel ratio based on SVM under two kinds of kernels were obtained as shown in table 4 and table 5.

Similarly, by exporting the training output data and verification output data of the SVM, the identification results of the

TABLE 5. Verification accuracy under temperature drop condition.

kernel	mse	rmse	mae	mre
poly(10s)	0.0016	0.0403	0.034	0.24%
poly(20s)	0.3561	0.5968	0.593	4.12%
rbf(10s)	0.0038	0.062	0.0484	0.34%
rbf(20s)	0.3219	0.5673	0.561	3.9%

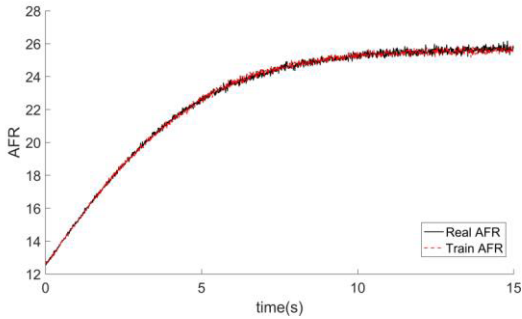


FIGURE 7. Training results of the air-fuel ratio under temperature drop condition.

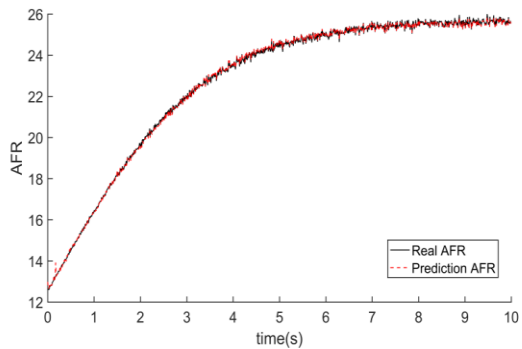


FIGURE 8. Validation results of the air-fuel ratio of 10s test datasets under temperature drop condition.

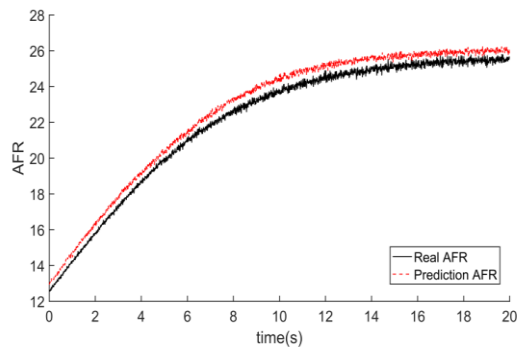


FIGURE 9. Validation results of air-fuel ratio of 20s test datasets under temperature drop condition.

air-fuel ratio can be obtained as shown in Fig. 7, Fig. 8 and Fig. 9 (The figures were obtained by selecting the data with highest accuracy in table 4 and table 5).

D. DISCUSSIONS OF IDENTIFICATION RESULTS

It can be seen from the accuracy data of table 2, table 3, table 4 and table 5 that for the air-fuel ratio identification of the HHHTS, the training accuracy of SVM is satisfactory in both cases under both polynomial and radial basis functions, and the training accuracy of SVM using polynomial as kernel function is slightly better than that using radial basis function as kernel function. When the training model was validated on the test datasets, it can be found that the validation accuracy and training accuracy are basically the same on the 10s test set. This shows that the air-fuel ratio identification model based on SVM has satisfactory accuracy. However, when it was validated on the 20s test datasets, the validation accuracy decreased greatly, because the data volume of the test datasets is larger than that of the training datasets, and it contains some new unknown features. This shows that in order to maintain satisfactory verification accuracy, the training datasets should be larger than the test datasets when using SVM for system identification. In addition, it can be clearly found from the figures (especially from figure 6 and figure 9) that when the value of the air-fuel ratio is low, the verification accuracy is high; the verification accuracy begins to decrease with the increase of the air-fuel ratio. This result is caused by the differences in the data itself, that is, from the actual air-fuel ratio curve in the figures, it can be seen that when the air-fuel ratio is low, the collected data is relatively smooth, with the increase of the air-fuel ratio, the smoothness of the collected data decreases, resulting in the decrease of the verification accuracy.

It also can be found from the accuracy data of table 2, table 3, table 4 and table 5 that although the parameters used by SVM have not changed during the identification of the temperature rise condition and temperature drop condition, the identification accuracy of the air-fuel ratio is different, that is, the training accuracy and verification accuracy under temperature rise condition are obviously better than that under temperature drop condition. This is due to the difference between the datasets. Comparing the air-fuel ratio curves of Fig 4 and Fig 7, it can be seen that the data collected under the temperature rise condition is smoother than that collected under the temperature drop condition, that is, the noise is smaller. This shows that SVM is sensitive to noise. When the noise contained in the data increases, the identification accuracy of the SVM will decrease. In addition, it can be found from the data in the tables that the average absolute error of the air-fuel ratio identification is not very different under the two working conditions, but the average relative error is quite different. This is due to the difference of the average value of the air-fuel ratio data under the two working conditions, that is, the average value of the air-fuel ratio under the temperature rise condition is higher than that under the temperature drop condition, which results in the average relative error increases obviously under the condition of the temperature drop condition.

In addition, it also can be found from the accuracy data of table 2, table 3, table 4 and table 5 that the accuracy of the

training and 10s test is slightly better when the polynomial function is used as the kernel function, however, the accuracy of 20s test is slightly better when the radial basis function is used as the kernel function. These results show that the ability of radial basis function to adapt to new data is better than that of polynomial kernel function.

V. CONCLUSION

In order to overcome the phenomenon of the fuel-rich combustion in the combustor of the HHHTS and improve the combustion efficiency and gas temperature control performance, this paper presented a method to identify the air-fuel ratio of the system, that is, to obtain the actual air-fuel ratio of the system by identifying the air-fuel ratio, and then adjust it to avoid fuel-rich combustion. In order to identify the air-fuel ratio of the system, this paper briefly analyzed the mathematical model of the air-fuel ratio of the test system, and proposed an air-fuel ratio identification method based on SVM. The air-fuel ratio of the system was identified by using different kernels based on the experimental data, and the following conclusions were obtained:

(1) When the test datasets are smaller than the training datasets, the SVM has a satisfactory identification performance in both polynomial kernel function and radial basis function. It can accurately approximate the actual dynamic process of the air-fuel ratio of the HHHTS. The average absolute error of the identification model is less than 0.05, and the average relative error is less than 0.5%. When the test datasets are larger than the training datasets, the identification accuracy of the SVM will be greatly reduced.

(2) For the identification of the air-fuel ratio of the HHHTS, on the 10s test datasets, the identification accuracy is better when the polynomial function is used as the kernel function, however, on 20s test datasets, the identification accuracy is better when the radial basis function is used as the kernel function.

(3) The identification accuracy of the air-fuel ratio based on SVM is sensitive to noise. When the noise contained in the datasets increases, the identification accuracy of the air-fuel ratio will decrease.

REFERENCES

- [1] C. Cai, Y. Li, and S. Dong, "Experimental study on gas temperature control for a high-speed heat-airflow wind tunnel," *J. Aerosp. Eng.*, vol. 29, no. 6, Nov. 2016, Art. no. 04016054.
- [2] C. Cai, Y. Yang, and T. Liu, "Coordinated control of fuel flow-rate for a high-temperature high-speed wind tunnel," *Proc. Inst. Mech. Eng., G, J. Aerosp. Eng.*, vol. 230, no. 13, pp. 2504–2514, Nov. 2016.
- [3] W. Xue, W. Bai, S. Yang, K. Song, Y. Huang, and H. Xie, "ADRC with adaptive extended state observer and its application to air-fuel ratio control in gasoline engines," *IEEE Trans. Ind. Electron.*, vol. 62, no. 9, pp. 5847–5857, Sep. 2015.
- [4] K. I. Wong and P. K. Wong, "Adaptive air-fuel ratio control of dual-injection engines under biofuel blends using extreme learning machine," *Energy Convers. Manage.*, vol. 165, pp. 66–75, Jun. 2018.
- [5] H.-M. Wu and R. Tafreshi, "Fuzzy sliding-mode strategy for air-fuel ratio control of lean-burn spark ignition engines," *Asian J. Control*, vol. 20, no. 1, pp. 149–158, Jan. 2018.
- [6] M. Kumar and T. Shen, "In-cylinder pressure-based air-fuel ratio control for lean burn operation mode of Si engines," *Energy*, vol. 120, pp. 106–116, Feb. 2017.
- [7] C. F. Aquito, "Transient A/F control characteristics of the 5 liter central fuel injection Engine," *SAE Trans.*, vol. 90, pp. 1819–1833, Feb. 1981.
- [8] D. Cho and J. K. Hedrick, "A nonlinear controller design method for fuel-injected automotive engines," *J. Eng. Gas Turbines Power*, vol. 110, no. 3, pp. 313–320, Jul. 1988.
- [9] E. Hendricks and S. C. Sorenson, "Mean value modeling of spark ignition engines," *SAE Trans.*, vol. 99, no. 3, pp. 1359–1373, Mar. 1990.
- [10] Z. Hou, Q. She, Y. Wu, H. Deng, and X. Yuan, "Air fuel ratio identification of gasoline engine during transient conditions based on elman neural network," *China J. Highway Transp.*, vol. 19, no. 6, pp. 113–117, Jun. 2006.
- [11] C. Linlin and W. Minxiang, "On transient air/fuel ratio control for gasoline engine on the basis of model identification," in *Proc. 27th Chin. Control Conf.*, Jul. 2008, pp. 355–359.
- [12] Z. Li and A. T. Shenton, "Nonlinear model structure identification of engine torque and air/fuel ratio," *6th IFAC Symp. Adv. Automot. Control*, Jul. 2010, pp. 709–714.
- [13] S. Saraswati and S. Chand, "Application of neural network for air-fuel ratio identification in spark ignition engine," *Int. J. Comput. Appl. Technol.*, vol. 32, no. 3, pp. 206–215, Mar. 2008.
- [14] Y. Shi, D.-L. Yu, Y. Tian, and Y. Shi, "Air-fuel ratio prediction and NMPC for Si engines with modified volterra model and RBF network," *Eng. Appl. Artif. Intell.*, vol. 45, pp. 313–324, Oct. 2015.
- [15] D. Xu, Y. Li, B. Liao, Z. Zhou, and P. Huang, "Study on the predictive model of chaotic support vector ma China for gasoline engine transient air-fuel ratio," in *Proc. 6th Int. Conf. Digit. Manuf. Automat.*, Jan. 2015, pp. 384–390.
- [16] Y. Zhai, K. L. Man, S. Lee, and F. Xue, "A neural network based soft sensor for air fuel ratio dynamics in SI engines," in *Proc. Int. Multi Conf. Eng. Comput. Sci.*, Mar. 2017, pp. 719–722.
- [17] T. Liu, S. Liang, Q. Xiong, and K. Wang, "Two-stage method for diagonal recurrent neural network identification of a high-power continuous microwave heating system," *Neural Process. Lett.*, vol. 50, no. 3, pp. 2161–2182, Dec. 2019.
- [18] X. Gao, S. Wang, R. Liu, and B. Sun, "Hopfield neural network identification for Prandtl-Ishlinskii hysteresis nonlinear system," in *Proc. Chin. Intell. Syst. Conf.*, Oct. 2018, pp. 153–161.
- [19] F. Martinelli, F. Mercaldo, V. Nardone, and A. Santone, "Car hacking identification through fuzzy logic algorithms," in *Proc. IEEE Int. Conf. Fuzzy Syst. (FUZZ-IEEE)*, Jul. 2017, pp. 1–7.
- [20] S. Saha, A. Gayen, H. R. Pourghasemi, and J. P. Tiefenbacher, "Identification of soil erosion-susceptible areas using fuzzy logic and analytical hierarchy process modeling in an agricultural watershed of burdwan district, india," *Environ. Earth Sci.*, vol. 78, no. 23, p. 649, Dec. 2019.
- [21] Y.-F. Jin, Z.-Y. Yin, S.-L. Shen, and D.-M. Zhang, "A new hybrid real-coded genetic algorithm and its application to parameters identification of soils," *Inverse Problems Sci. Eng.*, vol. 25, no. 9, pp. 1343–1366, Sep. 2017.
- [22] S.-P. Zhang and X.-K. Xin, "Pollutant source identification model for water pollution incidents in small straight rivers based on genetic algorithm," *Appl. Water Sci.*, vol. 7, no. 4, pp. 1955–1963, Jul. 2017.
- [23] W. Huang, J. Lu, H. Ye, W. Kong, A. H. Mortimer, and Y. Shi, "Quantitative identification of crop disease and nitrogen-water stress in winter wheat using continuous wavelet analysis," *Int. J. Agric. Biol. Eng.*, vol. 11, no. 2, pp. 145–152, Feb. 2018.
- [24] R. Ke, Z. Zeng, Z. Pu, and Y. Wang, "New framework for automatic identification and quantification of freeway bottlenecks based on wavelet analysis," *J. Transp. Eng., A, Syst.*, vol. 144, no. 9, Sep. 2018, Art. no. 04018044.
- [25] V. J. Nagalkar and G. G. Sarate, "Brain Tumor Detection and Identification using Support Vector Machine," *Int. Res. J. Eng. Technol.*, vol. 06, no. 12, pp. 2020–2023, Dec. 2019.
- [26] X. Hou, G. Wang, G. Su, X. Wang, and S. Nie, "Rapid identification of edible oil species using supervised support vector machine based on low-field nuclear magnetic resonance relaxation features," *Food Chem.*, vol. 280, pp. 139–145, May 2019.
- [27] R. Russo, G. Romano and P. Colombo "Identification of various control chart patterns using support vector machine and wavelet analysis," *Ann. Elect. Electron. Eng.*, vol. 2, no. 8, pp. 6–12, Aug. 2019.
- [28] E. Hendricks, A. Chevalier and M. Jensen, "Modeling of the intake manifold filling dynamics," *SAE Trans.*, vol. 105, no. 3, pp. 122–146, Mar. 1996.



CHAOZHI CAI received the B.S. and M.S. degrees in measurement and control technology and instrument from the Hebei University of Engineering, Handan, Hebei, China, in 2007 and 2010, respectively, and the Ph.D. degree in mechatronics engineering from Beihang University, Beijing, China, in 2014.

Since 2016, he has been an Associate Professor of mechanical engineering with the Hebei University of Engineering. He has published more than 20 refereed journal articles and conference papers in journals sponsored by the IEEE, SAGE, ASME, and other academic institutions. His research interests include process system modeling and control, hydraulic and mechatronic servo control, system identification, robot control, and artificial intelligence.



LUBIN GUO received the B.S. degree in mechatronic engineering from the Taiyuan Institute of Technology, China, in 2018. He is currently pursuing the M.S. degree with the College of Mechanical and Equipment Engineering, Hebei University of Engineering, China. His current research interests are in analysis and control of thermal systems.



YUMIN YANG received the B.S. degree from the Changchun University of Science and Technology, China, and the M.S. and Ph.D. degrees from Shanghai University. She is currently an Associate Professor with the Department of Mechatronics Engineering, Hebei University of Engineering. She has published extensively and holds numerous patents in her research areas. Her current research interests include control system design, and rotor system dynamics and control.

...